IR side of positivity bounds

Brando Bellazzini,[1,2,3] Marc Riembau[ORCID],[2] and Francesco Riva[4]

[1]*Université Paris-Saclay, CNRS, CEA, Institut de Physique Théorique, 91191 Gif-sur-Yvette, France*
[2]*Theoretical Particle Physics Laboratory (LPTP), Institute of Physics, EPFL, CH-1015 Lausanne, Switzerland*
[3]*CERN, Theoretical Physics Department, Esplanade des Particules 1, P.O. Box 1211 Geneva, Switzerland*
[4]*Départment de Physique Théorique, Université de Genève,*
24 quai Ernest-Ansermet, 1211 Genève 4, Switzerland

We show how calculable IR loop effects impact positivity bounds in effective field theories with causal and unitary UV completions. We identify infrared singularities that appear in dispersion relations at $|t| \lesssim m^2$. In the massless limit, they weaken two-sided bounds based on crossing symmetry, such as the lower bound on the amplitude for Galileon scattering. For amplitudes that are analytic in s even for large negative t, i.e., $|t| \gg m^2$, we propose a new simple analytic approach to dispersive bounds, which are instead insensitive to the singularities, and explicitly compute the finite contributions from loops. Finally, we show that the singularity do not affect the bounds based on smearing in the impact parameter.

I. INTRODUCTION

The space of low-energy relativistic effective field theories (EFTs) is subject to fundamental constraints known as positivity bounds. They encode, in the form of inequalities among scattering amplitudes evaluated in the infrared (IR), the conditions that EFTs emerge from the renormalization-group (RG) evolution of unitary and causal microscopic dynamics. IR-consistent EFTs failing the positivity bounds belong to the "swampland."

Positivity bounds stem from dispersion relations that provide this UV and IR connection [1–3]. While rooted in the old S-matrix bootstrap, the deeper understanding and implications of positivity bounds were put forward in [4], where the connection with the requirement of subluminal propagation of the low-energy degrees of freedom was also made explicit.

Generalization to arbitrary spinning particles [5,6] and to finite scattering angle [7–10], along with interesting applications in particle phenomenology [9,11–25], and in gravitational physics [26–36], or in connection to the positivity of time delay [37–39], have recently led to the uncovering of the architecture behind all positivity bounds, (called EFT-Hedron in [40]), where infinitely many Wilson coefficients are constrained, at tree level, by double-sided bounds [40–47].

The chief purpose of this article is to show how calculable IR effects and loops deform the EFT-Hedron beyond the idealized tree-level limit. Discussing realistic EFTs at finite coupling in the IR is important in order to render positivity bounds actually sharp: Throwing theories in the swampland must be irreversible and should not be undone by weak coupling corrections possibly enhanced by IR divergences.

Broadly speaking, there are two implications of IR loop effects on positivity bounds for Wilson coefficients, when evaluated at the EFT cutoff where two-sided bounds are most relevant. First of all, n-subtracted dispersion relations involve (via the integral along the IR discontinuity) all EFT couplings, in contrast to the tree-level limit where they select the coefficient of s^n in the amplitude. Therefore, sharp dispersive bounds deliver not so sharp constraints on Wilson coefficients and, for practical applications, require perturbative assumptions about the EFT convergence [41]. Secondly, and perhaps more importantly, in the massless limit, the nonanalyticities extend to $s \to 0$ and $t \to 0$. There, the most relevant interactions and their IR loops always dominate the amplitude, screening, potentially, information on less relevant couplings. Moreover, the amplitude being nonanalytic in t as the mass goes to zero restricts the use of the dispersion relations based on the near-forward region.

In this article, we present a thorough study of one-loop effects within the EFT of a scalar with four-point interactions, focusing on forward singularities and their impact on two-sided bounds. As a case study, we discuss bounds on the ratio $g_{3,1}s/g_2$ between the coefficients $g_{3,1}$ of stu in the amplitude (which would be dominant for
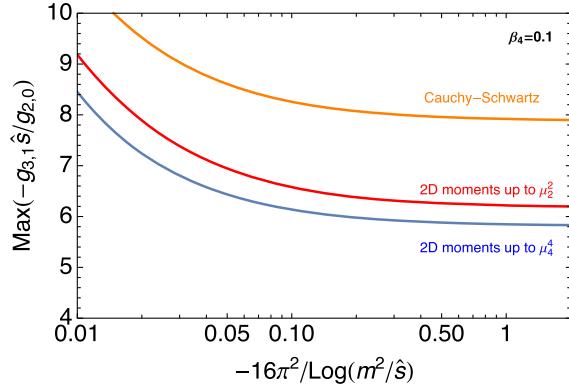
FIG. 1. Bounds on ratio $g_{3,1}\hat{s}/g_{2,0}$ as a function of the particle mass m, for fixed $\beta_4\hat{s}^2 = 0.1$. Lower lying curves correspond to bounds involving more moments in the UV: in orange only Cauchy-Schwartz Eq. (33), in red moments up to μ_2^2 as in Eq. (28), and in blue moments up to μ_4^4 (numerical). All curves diverge as $m \to 0$.

Galileons [48]) and the coefficient g_2 of $s^2 + t^2 + u^2$ (ordinary Goldstone boson) and discuss how the arguments generalize to other couplings.

Expressing *near-forward* $t \approx 0$ dispersion relations as 2D moments of a positive measure in the UV, generalizing [41] along the lines of [46], we show that the lower bound on $g_{3,1}s/g_2$ that holds at tree level actually disappears, in the massless limit, regardless of how small the coupling is taken, as shown in Fig. 1. The same conclusion holds for the approaches of Refs. [40,42,43].

This pessimistic result is, however, based on the near-forward positivity bounds only, which posit amplitude's analyticity only within the rigorously proven domain. We contrast such conclusions with those we obtain by working with an enlarged domain of analyticity in s for negative $t \ll -m^2$, which, despite not being rigorously proved, is supported by the perturbative analysis of Landau equations within the EFT. We present a simple approach to dispersion relations that shows that the tree-level bounds do actually survive also at loop level, as long as the coupling remains perturbative, under the assumption of maximal analyticity. Our approach is analytic and simple and nicely complements the numerical technique of [45].

II. DISPERSION RELATIONS AT FINITE t

We study $2 \to 2$ scattering of a single particle of spin-0. We assume that the amplitude $\mathcal{M}(s,t)$ is analytic in the entire complex s plane except the physical branch cut at $s \geq 4m^2$ and its crossing symmetric counterpart at $s < -t$, for fixed values of t as specified in the following sections. We focus on the amplitude with $n + 2$ $(n \geq 0)$ subtractions in $s = 0$ and $n + 1$ subtractions in $s = -t$ and define "arcs" the following $\hat{s}$- and t-dependent contour integral

$$a_n(\hat{s}, t) \equiv \int_{\smile}^{\frown} \frac{d\hat{s}'}{2\pi i \hat{s}'} \frac{\hat{\mathcal{M}}(\hat{s}', t)}{[\hat{s}'(\hat{s}' + t)]^{n+1}}, \quad n \geq 0, \quad (1)$$

where

$$\hat{s} \equiv s - 2m^2, \qquad \hat{\mathcal{M}}(\hat{s}, t) \equiv \mathcal{M}(s, t), \quad (2)$$

and $\overset{\frown}{\smile}$ is the circle with radius $\hat{s} + t/2$ and centered at $-t/2$ (minus its interception with the real axis). Arcs probe the theory at energy $\hat{s}$ and momentum transfer $q^2 = -t$ and are suited to capture the RG flow within EFTs.

We deform the contour $\overset{\frown}{\smile}$ into a contour that encompasses the discontinuities on positive $\hat{s}' \geq \hat{s}$ and negative $\hat{s}' \leq -\hat{s} - t$ real axis, together with upper and lower semicircles at infinity. We further assume that the latter vanish, because

$$\lim_{|s| \to \infty} \mathcal{M}(s, t)/s^2 = 0, \quad (3)$$

as implied by the Froissart-Martin bound [49–51]. From crossing symmetry, real analyticity, and the partial-wave expansion,

$$\hat{\mathcal{M}}(\hat{s}, t) = \hat{\mathcal{M}}(-\hat{s} - t, t), \qquad \hat{\mathcal{M}}(\hat{s}, t) = \hat{\mathcal{M}}^*(\hat{s}^*, t),$$

$$\hat{\mathcal{M}}(\hat{s}, t) = \sum_{l=0}^{\infty} P_\ell\left(1 + \frac{2t}{\hat{s} - 2m^2}\right)\hat{f}_\ell(\hat{s}), \quad (4)$$

where $P_\ell(\cos\theta)$ are the Legendre polynomials, and ℓ is even for identical scalars, we can express the *arcs* in terms of their UV integral representation,

$$a_n(\hat{s}, t) = \frac{2}{\pi} \int_{\hat{s}}^{\infty} \sum_{\ell=0}^{\infty} d\hat{s}' \mathrm{Im}\hat{f}_\ell(\hat{s}') \frac{I_t^n(\ell, \hat{s}')}{\hat{s}'^{2n+3}}, \quad (5)$$

with the kernel $I_t^n(\ell, \hat{s}')$ given by

$$I_t^n(\ell, \hat{s}') \equiv \frac{(1 + \frac{t}{2\hat{s}'})}{(1 + \frac{t}{\hat{s}'})^{n+2}} P_\ell\left(1 + \frac{2t}{\hat{s}' - 2m^2}\right). \quad (6)$$

In the following, we are interested in the limit

$$m^2 \ll s, \quad (7)$$

where also $\hat{s} \to s$. In practice, we will set $m \to 0$ everywhere except in the presence of IR divergences where the mass acts as an explicit regulator.

A. IR Arcs

Arcs can be computed within the EFT via Eq. (1) in terms of Wilson coefficients. Consider an EFT which, in a weak-coupling regime, can be well approximated by the tree-level expression,

$$\mathcal{M}(s,t) = \sum_{n,q} g_{n,q} \left(\frac{s^2 + t^2 + u^2}{2} \right)^{\frac{n-3q}{2}} \cdot (stu)^q, \quad (8)$$

where n sets the overall energy-squared scaling, whereas q tells how fast the amplitude vanishes for $t \to 0$ and fixed s. Then, at $t = 0$, the arcs read

$$a_n(\hat{s}, 0) = g_{2n+2,0}, \quad (9)$$

while at finite t,[1]

$$a_0(\hat{s}, t) = \sum_{n=1}^{\infty} \left[n t^{2n-2} g_{2n,0} - t^{2n-1} g_{2n+1,1} \right], \quad (10)$$

with similar expressions for higher arcs. At tree level, arcs are in one-to-one correspondence with couplings. In particular, knowledge of

$$a_n|_{t=0}, \partial_t a_n|_{t=0}, \dots, \partial_t^{n+1} a_n|_{t=0} \quad (11)$$

is enough to reconstruct the whole series of Wilson coefficients.

From Eq. (8), IR loop effects are calculable. In this article, we will focus on the most important one-loop effect, from two insertions of $g_{2,0}$:

$$\delta\mathcal{M} = \frac{\beta_4}{2} s^2 \left(s^2 - \frac{tu}{21} \right) \log(-s) + (s \leftrightarrow t, u), \quad (12)$$

where the renormalization scale is implicit, and

$$\beta_4 = -\frac{7}{10} \frac{g_{2,0}^2}{16\pi^2}, \quad (13)$$

which must be small $|\beta_4 \hat{s}^2| \ll 1$ for the perturbative expansion to make sense. This gives an additional contribution to the first arc,

$$\delta a_0(\hat{s}, t) = \beta_4 \left(\hat{s}^2 - \frac{41}{21} \hat{s} t + \frac{t^2}{2} - \frac{\hat{s}^3}{2(\hat{s} + t)} \right. \\ \left. + t^2 \left(2 \log(\hat{s} + t) + \frac{1}{42} \log \frac{-t}{\hat{s} + t} \right) \right), \quad (14)$$

which is nonanalytic in either $s, t, u \to 0$. In particular, the term proportional to $t^2 \log -t$ will play an important role in what follows, since present bounds rely on arc t-derivatives in the forward limit, $\partial_t^m a_n|_{t=0}$. In fact, all couplings generate nonanalyticities in $t = 0$. The most singular effects in the one-loop contributions proportional to the marginal coupling $g_{0,0}$ are

$$\delta\mathcal{M} = \frac{g_{0,0}}{32\pi^2} \log \frac{-t}{s} \left(-g_{0,0} + t^2 \frac{5g_{2,0}}{3} \right. \\ \left. + t^3 \frac{g_{3,1}}{3} + t^4 \frac{7g_{4,0}}{5} + \cdots \right). \quad (15)$$

These (and all other one-loop contributions involving $g_{0,0}$) carry no powers of s and therefore, do not appear in arcs and do not enter in the dispersion relations.

On the other hand, one-loop effects involving less relevant couplings have singularities:

$$\delta\mathcal{M} = -\frac{s^2 t^2}{16\pi^2} \log \frac{-t}{s} \left(-t \frac{g_{2,0}g_{3,1}}{30} + t^2 \frac{2g_{2,0}g_{4,0}}{35} \right. \\ \left. + t^2 \frac{g_{3,1}g_{3,1}}{60} - t^3 \frac{2g_{3,1}g_{4,0}}{35} + t^2 s^2 \frac{g_{4,0}^2}{1260} + \cdots \right).$$

Of these, the first four will appear in the first arc $a_0(s,t)$ and will be subdominant to the term $\propto g_{2,0}^2$ from Eq. (14). Only the term $\propto g_{4,0}^2$ has enough powers of s to appear in the second arc a_1, but it is proportional to $t^4 \log(-t)$. Therefore, the second arc and its first three derivatives are regular at $t \to 0$. This trend propagates to higher arcs, with leading divergences,

$$\delta a_n(\hat{s}, t) \propto t^{2n+2} \log \frac{-t}{\hat{s}}. \quad (16)$$

We deduce that arc n and its first $2n + 1$ derivatives are regular in $t \to 0$. This is important in light of Eq. (11): It is possible to reconstruct all coefficients in the forward limit, without encountering $t = 0$ singularities.[2] We illustrate this in Table I.

III. 2D MOMENTS AND DISPERSION RELATIONS AROUND $t = 0$

We now discuss bounds on arcs and how they translate to bounds on Wilson coefficients, given the results of the previous section. In this first section, we take a conservative approach and rely only on analyticity of the amplitude for t within the domain established (assuming unitarity) by Martin [52–54], whose size is set by the scattered particle mass m. In the limit of small mass $m \to 0$, which we consider here, analyticity requires $t \to 0$.

---

[1]The subtraction choice $\frac{1}{[s(s+t)]^{n+1}} = \frac{(-t)^{n+1}}{(stu)^{n+1}}$ in Eq. (1) implies that the coefficient of $(stu)^q$ only appears in $a_{n\geq q-1}$, while $(s^2 + t^2 + u^2)^p$ appears in all $a_{n\leq p}$. This coincides with the choice of Ref. [41] only at $t = 0$.

[2]Note that the pattern of IR divergences Eq. (16) translates into a pattern of UV divergences, as $\partial_t^{(k)} a_n(\hat{s}, t)|_{t=0}$ is mapped to a UV integral proportional to $\sum_\ell \ell^{2k}/s^n$. At fixed n, for high enough k, the IR part diverges, implying a measure with support on arbitrarily large ℓ. At fixed k, for high enough n, the IR converges, implying that contributions from large ℓ also have large s. With the ansatz $m^2 \sim \ell^\alpha$ for the UV spectrum, Eq. (16) fixes $\alpha = 2$ exactly ($\alpha = 1$ would correspond to $a_n(\hat{s}, t) \propto t^{n+1} \log \frac{-t}{\hat{s}}$).

TABLE I. In bold, a schematic representation of the arcs and their derivatives (both at $t = 0$) needed to reconstruct all Wilson coefficients, Eq. (11). Italic cells correspond instead to arc derivatives that are singular at $t = 0$, according to Eq. (16).

a_0	$\partial_t a_0$	$\partial_t^2 a_0$	$\partial_t^3 a_0$	$\partial_t^4 a_0$	$\partial_t^5 a_0$	$\cdots$
a_1	$\partial_t a_1$	$\partial_t^2 a_1$	$\partial_t^3 a_1$	$\partial_t^4 a_1$	$\partial_t^5 a_1$	$\cdots$
a_2	$\partial_t a_2$	$\partial_t^2 a_2$	$\partial_t^3 a_2$	$\partial_t^4 a_2$	$\partial_t^5 a_2$	$\cdots$
a_3	$\partial_t a_3$	$\partial_t^2 a_3$	$\partial_t^3 a_3$	$\partial_t^4 a_3$	$\partial_t^5 a_3$	$\cdots$
$\vdots$	$\vdots$	$\vdots$	$\vdots$	$\vdots$	$\vdots$	$\ddots$

One efficient way of deriving near-forward bounds, involves mapping UV arcs to moments of a positive distribution in $\hat{s}$ and ℓ [41,46]. Bounds on moments then provide bounds from the UV; see [46,55]. The interpretation in terms of moments is possible because the coefficients in the t-Taylor expansion of the arc integrand Eq. (6) are themselves polynomials in $1/\hat{s}'$ and $J^2 \equiv \ell(\ell+1)$,

$$I_t^n(\ell, \hat{s}') = \sum_{m=0}^{\infty} \left(\frac{t}{\hat{s}'}\right)^m \sum_{k=0}^{m} d_{n,m-k} \sum_{i=0}^{k} \alpha_i^k J^{2i}, \quad (17)$$

with

$$d_{n,i} \equiv (-1)^i \frac{(i+n)!}{i!n!} \frac{2n+i+2}{2n+2}, \quad (18)$$

$$\sum_{i=0}^{k} \alpha_i^k J^{2i} \equiv \frac{1}{(k!)^2} \prod_{j=0}^{k-1} (J^2 - j(j+1)), \quad (19)$$

from expanding, respectively, the ratio and Legendre polynomials in Eq. (6). Changing variables,

$$x = (\hat{s}/\hat{s}'), \quad (20)$$

we can thus write the arc t-derivatives as linear combinations,

$$\frac{1}{m!}\partial_t^m a_n(t, s)\big|_{t=0} = \sum_{k=0}^{m} d_{n,m-k} \sum_{j=0}^{k} \alpha_j^k \mu_{2n+m}^j, \quad (21)$$

of two-dimensional moments,

$$\mu_n^q = \frac{1}{\hat{s}^{n+2}} \int d\mu(x, J^2) x^n J^{2q}, \quad (22)$$

with respect to a positive measure $d\mu(x, J^2)$ (proportional to $x \mathrm{Im}\hat{f}_{\ell(J^2)}(\hat{s}/x)dx > 0$ by unitarity) with support on $x \in [0, 1]$, times the noncompact discrete set of positive integer numbers (for even ℓ, $J^2 = 0, 6, 20, \ldots$). More explicitly, the arcs $a_n(\hat{s}, t)$ at finite t are written via their UV representation as linear combinations of 2D moments,

$$a_n(\hat{s}, t) = \mu_{2n}^0 + t\left(\mu_{2n+1}^1 - \frac{3+n}{2}\mu_{2n+1}^0\right)$$
$$+ t^2\left(\frac{\mu_{2n+2}^2}{4} - (2+n)\mu_{2n+2}^1 + \frac{(2+n)^2}{2}\mu_{2n+2}^0\right)$$
$$+ \cdots, \quad (23)$$

where dots denote higher powers of t.

A. Bounds on moments

Once arcs are expressed in terms of moments, their positivity constraints stem from the bounds on the 2D moments, which, in turn, are in one-to-one correspondence with the space of all polynomials in x and J^2 that are positive on the integration domain. Indeed, every positive polynomial $\sum \bar{\beta}_{i,j} x^i J^{2j} \equiv p(x, J^2) > 0$ implies a positivity condition among moments, $\sum \beta_{i,j} \mu_i^j = \int d\mu(x, J^2) p(x, J^2) > 0$.

We will first take the limit in which J^2 is continuous, which allows us to find *conservative* bounds in terms of a *finite* number of conditions. The continuum bounds (which are quantitatively very similar to exact bounds) will be more conservative because the space of positive polynomials in the continuum contains those positive in the discrete. Moreover, this approach will enable us to obtain analytic bounds without having to rely on numerical extrapolations to large ℓ. In Appendix, we will show how to include the countably infinite conditions that define the bounds for ℓ discrete.

The set $(x, J^2) \in [0, 1] \times \mathbb{R}^+$ can be described by the conditions,

$$x \geq 0, \qquad 1 - x \geq 0, \qquad xJ^2 \geq 0. \quad (24)$$

From this, a theorem due to Schmüdgen [55,56] classifies all positive polynomials $p(x, J^2)$ in a domain in terms of squares of polynomials as[3]

$$p(x, xJ^2) = \sum_k q_k(x, J^2)\left(\sum_{i,j} \beta_{i,j}^k x^{i+j} J^{2j}\right)^2, \quad (25)$$

where q_k stem from products of the monomials in Eq. (24) defining the domain as $q_k \geq 0$, and in our case, belongs to the set,

$$\{1, x, xJ^2, J^2x^2, 1-x, x(1-x), J^2x(1-x), J^2x^2(1-x)\}.$$

These capture terms that cannot be written as squares (recall J^2 rather than J is the variable entering in the

---

[3]Eqs. (24), (25) parametrize polynomials of (x, xJ^2) rather than (x, J^2). This is an efficient set of polynomials to characterize moments μ_n^q with $n \geq q$, as they appear in arcs Eq. (21). It will provide simpler expression when considering truncations to polynomials of finite order (a finite number of moments) but does not make any difference once polynomials of arbitrary order are taken into account.

polynomials). The conditions for each individual q_k can be written in compact form. For instance, for $q_k = 1$, integrating Eq. (25) against the positive measure leads to the condition $\sum_{i,j,m,n} \beta^1_{i,j} \mu^{j+n}_{i+j+m+n} \beta^1_{m,n} > 0$, which implies positive definiteness of the infinitely sized matrix,

$$
H_{(0,0)} =
\left(
\begin{array}{c|cc|ccc|c}
\mu^0_0 & \mu^0_1 & \mu^1_1 & \mu^0_2 & \mu^1_2 & \mu^2_2 & \cdots \\
\hline
\mu^0_1 & \mu^0_2 & \mu^1_2 & \mu^0_3 & \mu^1_3 & \mu^2_3 & \cdots \\
\mu^1_1 & \mu^1_2 & \mu^2_2 & \mu^1_3 & \mu^2_3 & \mu^3_3 & \cdots \\
\hline
\mu^0_2 & \mu^0_3 & \mu^1_3 & \mu^0_4 & \mu^1_4 & \mu^2_4 & \cdots \\
\mu^1_2 & \mu^1_3 & \mu^2_3 & \mu^1_4 & \mu^2_4 & \mu^3_4 & \cdots \\
\mu^2_2 & \mu^2_3 & \mu^3_3 & \mu^2_4 & \mu^3_4 & \mu^4_4 & \cdots \\
\hline
\cdots & \cdots & \cdots & \cdots & \cdots & \cdots & \cdots
\end{array}
\right)
\succ 0,
$$

(26)

where the indices of $H_{(0,0)}$ denote the indices of the first entry, and the blocks correspond to monomials of given order k in x: $x^{k-i}(xJ^2)^i$, $i = 0, \ldots, k$.

Taking into account the other q_k, we find the conditions on the shifted matrices,

$$
H_{(0,0)} \succ 0 \qquad H_{(1,0)} \succ 0 \qquad H_{(1,1)} \succ 0 \qquad H_{(2,1)} \succ 0
$$
$$
H_{(0,0)} - \hat{s}^2 H_{(1,0)} \succ 0, \qquad H_{(1,0)} - \hat{s}^2 H_{(2,0)} \succ 0,
$$
$$
H_{(1,1)} - \hat{s}^2 H_{(2,1)} \succ 0.
$$

(27)

Contrary to the 1D moment problem [39], in 2D and higher, there is no optimal solution involving only a finite number of moments (the truncated 2D moment problem is solved only asymptotically). This means that in order to find the exact bounds satisfied by, e.g., moments up to order two in x and xJ^2, $\{\mu^0_0, \mu^0_1, \mu^1_1, \mu^0_2, \mu^1_2, \mu^2_2\}$, we still need to compute infinitely many bounds involving infinitely many moments and then project into the finite subset. Because of Sylvester's criterion, positive definiteness in Eq. (27) implies also positive definiteness of all finite-size principal minors, corresponding to matrices $H_{(i,j)}$ of finite size. This necessary but not sufficient condition leads to conservative bounds. For instance, the bounds in Eq. (26) involving only moments up to μ^2_2 are

$$
\begin{pmatrix}
\mu^0_0 & \mu^0_1 & \mu^1_1 \\
\mu^0_1 & \mu^0_2 & \mu^1_2 \\
\mu^1_1 & \mu^1_2 & \mu^2_2
\end{pmatrix}
\succ 0 \qquad \mu^0_1 > 0 \qquad \mu^1_1 > 0 \qquad \mu^1_2 > 0
$$
$$
\mu^0_0 - \hat{s}^2 \mu^0_1 > 0 \qquad \mu^0_1 - \hat{s}^2 \mu^0_2 > 0 \qquad \mu^1_1 - \hat{s}^2 \mu^1_2 > 0, \quad (28)
$$

and represent a simple (albeit not optimal) subset of all bounds.

B. Bounds on Wilson coefficients

Now, near-forward bounds on Wilson coefficients stem from comparing, order by order in t, IR and UV definitions of arcs in terms of moments. Using Eq. (10) and expanding the loop contribution Eq. (14), we find from $a_0(\hat{s}, t)$,

$$
g_{2,0} + \frac{\beta_4 \hat{s}^2}{2} = \mu^0_0, \qquad -g_{3,1} - \frac{61}{42}\beta_4 \hat{s} = \mu^1_1 - \frac{3}{2}\mu^0_1,
$$
$$
2g_{4,0} + \beta_4 \left(2\log \hat{s} + \frac{\log(m^2/\hat{s})}{42}\right) = \frac{\mu^2_2}{4} - 2\mu^1_2 + 2\mu^0_2. \quad (29)
$$

The term proportional to $\log m^2$ represents the leading effect at finite mass, which acts here as a regulator for the otherwise divergent expression as $t \to 0$.

From Eq. (28) (in particular, $\mu^1_1 > 0$ and $\mu^0_0 - \hat{s}^2 \mu^0_1 > 0$), we read the upper bound

$$
g_{3,1}\hat{s} < \frac{3}{2}g_{2,0} - \frac{10}{7}\beta_4 \hat{s}^2, \quad (30)
$$

which, for $\beta_4 \to 0$, reduces to the tree-level values discussed in [10,41].

On the other hand, the moments μ^1_1, μ^2_2 do not have upper bounds in Eq. (28), and consequently there appears to be no lower bound on $g_{3,1}$.[4] A lower bound stems from realizing that, because of full $s - t - u$ crossing symmetry [42,45], $g_{4,0}$ appears also in the second arc at $t = 0$,

$$
a_1 = g_{4,0} + \beta_4 \log \hat{s} = \mu^0_2. \quad (31)
$$

Comparing this to the second line in Eq. (29) leads to a null constraint which, taking into account loop effects, reads

$$
\mu^2_2 = 8\mu^1_2 + \frac{2\beta_4}{21}\log\frac{m^2}{\hat{s}}. \quad (32)
$$

Null constraints relate higher and lower moments in J^2 and, together with bounds on moments, lead also to a lower bound on $g_{3,1}$ [42–44,46]. The simplest way to see this is to combine the null constraint with the condition $\mu^1_1 - \hat{s}^2 \mu^0_2 > 0$ and $\mu^2_2 \mu^0_0 > (\mu^1_1)^2$ [the latter follows from positivity of the minors in the positive definite matrix of Eq. (28)] to obtain

$$
g_{3,0}\hat{s} > -4g_{2,0}\left(1 + \sqrt{1 - \frac{g_{2,0}\hat{s}^2 \log\frac{m^2}{\hat{s}}}{240 \times 16\pi^2}}\right) - \frac{10}{7}\beta_4 \hat{s}^2. \quad (33)
$$

In absence of loop effects, this reduces to $g_{3,0}\hat{s} > -8g_{2,0}$; instead, using all relations from Eq. (28), we find $g_{3,0}\hat{s} > -6.5g_{2,0}$; finally, using moments up to μ^6_6, we find

---

[4]This is a consequence of the ℓ domain being noncompact: μ^q_n can be larger and larger as q increases. In contrast, $0 \leq x \leq 1$, and moments μ^q_n are monotonically decreasing in n.

$g_{3,0}\hat{s} \gtrsim -5.3g_{2,0}$ in agreement with [42–44,46]—this is an example of how the 2D moment problem converges as more and more moments are taken into account.

We show these bounds, as function of $\log m^2\hat{s}$, in Fig. 1.[5] The interesting feature is that in the exact $m = 0$ limit, although the upper bound is untouched, the lower bound disappears completely.

Nevertheless, for practical purposes, in the case of the Goldstone, as soon as the mass is finite, the impact of loop effects is limited. Indeed, even considering the most favorable phenomenological conditions for the EFT, in which the cutoff is at the Planck scale $\hat{s} = M_{pl}^2$, while the mass of the particle is at the lowest testable scale (Hubble) $m = H_0$, the logarithm is of order $\log \frac{m^2}{\hat{s}} \approx -280$, and the departures from the tree-level limit are of the size of a loop factor $\sim g_{2,0}^2 s^2/16\pi^2$.

In the approach of this section, positive functions are approximated by polynomials. This is a strength because they provide a simple and systematic path to positivity. At the same time, polynomials are the weak link of this approach, as they do not converge uniformly to continuum functions on noncompact domains. For instance, consider the combination of moments associated with integrating $\cos J^2$ over the measure $d\mu$ in Eq. (22), $\mu^{\cos} \equiv \sum_{n=0}^{\infty}(-1)^n\mu_0^{2n}/(2n!)$. Clearly, $\mu^{\cos} < \mu_0^0$, since $|\cos J^2| < 1$; yet this feature is invisible at any finite order of moments. In the next section, we provide an alternative method to extract bounds that attacks directly the integrand boundedness.

IV. DISPERSION RELATIONS AT LARGE $-t$

In this section, we assume the amplitude to be analytic in the cut complex s plane for fixed large negative t (within the EFT validity)—as often (though not always [57]) assumed in the modern S-matrix bootstrap approach [58–60]. This provides a way of regulating the singularities using finite t rather than mass. Analyticity in s for finite $t < 0$ has been rigorously proven [61], except for a region of size $\sim(-t)^3$ around the origin. For t within the range of EFT validity, the amplitude is explicitly calculable and known, and it displays in fact no nonanalyticity.

The extended domain of analyticity enables us to study dispersion relations at fixed large negative t, without the need to expand them around $t \approx 0$. Unfortunately, contrary to analogous quantities defined at $t = 0$, Legendre polynomials are not positive, and therefore, the integrand Eq. (5) is *not positive*. For $-\hat{s} < t \leq 0$, however, the

integrand $I_t(\ell, \hat{s}')$ is *bounded from above and below*, because the Legendre polynomials are themselves bounded for all even ℓ and $\hat{s}' \in [\hat{s}, \infty[$,

$$-\frac{1}{2} \leq \min_{\ell,\hat{s}'}P_\ell\left(1 + \frac{2t}{\hat{s}' - 2m^2}\right) \leq P_\ell(\cos\theta) \leq 1. \quad (34)$$

Since the integrand is bounded, we can pull it out of the integral and bound arcs $a_n(\hat{s}, t')$ in terms of arcs at $t = 0$ (where $P_\ell(\cos\theta) = P_\ell(1) = 1$),

$$a_n(\hat{s}, 0) = \frac{2}{\pi}\int_{\hat{s}}^{\infty}\sum_{\ell=0}^{\infty}\frac{d\hat{s}'\mathrm{Im}\hat{f}_\ell(\hat{s}')}{\hat{s}'^{2n+3}} = \mu_{2n}^0, \quad (35)$$

which, as shown above, are strictly positive moments of a 1D distribution [41].

Combining Eqs. (5)–(35), we find the constraint,

$$\min_{\ell,\hat{s}'}I_t^n(\ell, \hat{s}') \leq \frac{a_n(\hat{s}, t)}{a_n(\hat{s}, 0)} \leq \frac{1 + t/(2\hat{s})}{(1 + t/\hat{s})^{n+2}}. \quad (36)$$

Here, for all t, the upper bound is exactly saturated in $\ell = 0$ or $\hat{s}' \to \infty$ (corresponding to $\cos\theta = 1$), $P_0(\cos\theta) = P_\ell(1) = 1$. Instead, for the generic value of $t/\hat{s}$, the lower bound is determined by different points in the $\ell, \hat{s}'$ domain: For $t/\hat{s} \sim -1/2$, $\min_{\ell,\hat{s}'} I_t(\ell, \hat{s}')$ is saturated by the $\ell = 2$ polynomial, and as $t/\hat{s} \to 0$ or 1, it is saturated by larger and larger values of ℓ.

The region excluded is illustrated for $n = 0$ by the gray area in Fig. 2 (the black lines correspond to the simple t-independent bound $-\frac{1}{2} \leq P_\ell(\cos\theta) \leq 1$).

We can now compare the arcs computed within the EFT Eq. (10) with the arcs bounded by UV unitarity and causality in Eq. (36). Calling s_{max} the theory's cutoff, we will first consider the kinematics,

$$|t| \ll \hat{s} \ll \hat{s}_{max}. \quad (37)$$

The second inequality labels the regime where loop effects are under control, even in strongly coupled theories.

We first discuss the tree-level limit in which we neglect these effects altogether such that the IR amplitude is well described by Eq. (8). We then invoke the first inequality in Eq. (37) so that the first arc is well approximated by

$$a_0(\hat{s}, t) \approx g_{2,0} - tg_{3,1}, \quad (38)$$

and higher-order terms can be neglected.[6]

---

[5]At fixed m, with more moments, the lower bound improves because the solution to the 2D moment problem is more precise, but it still diverges as $m \to 0$. In contrast to the tree-level limit, here higher null constraints [from expressing any $g_{p,q}$ in terms of different combinations of moments, similarly to Eq. (32)] do not improve the bound, because higher t-derivatives of Eq. (14) are more and more singular $\partial_t^k a_0 \sim m^{-2(k-2)}$ as $m \to 0$.

[6]While neglecting higher orders is a customary assumption in the context of EFTs, it is plausible that $g_{3,1}$ is not suppressed w.r.t. $g_{2,0}$ in units of $\hat{s}$, while higher-order terms are: a situation that corresponds to a system with approximate Galileon symmetry). This is possibility that we are exploring under assumption Eq. (38).
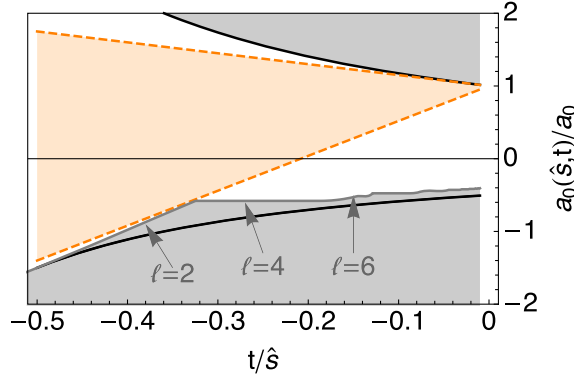
FIG. 2. Bounds on arc $a_0(\hat{s}, t)$ as a function of t. In gray, the region excluded by UV positivity bounds [in black, the region excluded by the simple approximation on the extremes of Eq. (34)]. Orange dashed lines illustrate IR arcs calculated with the approximated EFT ($a_0(\hat{s}, t)$ in Eq. (10) truncated at $O(t)$), for extremal values of $g_{3,1}$.

FIG. 3. Bounds on the ratio $g_{3,1}\hat{s}/g_{2,0}$ as a function of the coupling $g_{2,0}\hat{s}^2$. Gray area and dashed line: bounds neglecting terms $O(t^2)$ in $a_0(\hat{s}, t)$ [but using the full loop contribution Eq. (14)]. Solid lines: bounds from improved arcs, adding Eqs. (44) and (47).

The approximate IR tree-level EFT arc is illustrated in Fig. 2, by lines with steepness $-\hat{s}g_{3,1}/g_{2,0}$: Its extrema (orange dashed) are found by requiring that $a_0(\hat{s}, t)$ lies within the UV allowed region Eq. (36) for all values of $-1 \leq t/\hat{s} \leq 0$. Equating IR and UV arcs and dividing by $a_0(\hat{s}, 0)$, we find

$$\frac{3}{2} > \hat{s}\frac{g_{3,1}}{g_{2,0}} > -\min_t\left(\frac{\min\limits_{\ell,\hat{s}'} I_t^0 - 1}{-t}\right). \quad (39)$$

The upper bound is saturated by the $\ell = 0$, $\hat{s}' = \hat{s}$ UV contribution, corresponding to a weakly coupled scalar with mass $M^2 = \hat{s}$. This bound comes from the near-forward limit, where our assumption of neglecting higher-order terms is exact. It can be found analytically by comparing $\partial|_{t=0}a_0(\hat{s}, t)$ in the UV [the rhs of Eq. (36)] and the IR, Eq. (38), and is in fact equivalent to the moment problem approach.

The lower bound instead requires $\min_{\ell,\hat{s}'} I_t^0$, which implies finding the minima of (Legendre) polynomials, which is saturated by larger ℓ as $t/\hat{s} \to 0$. Nevertheless, the bound Eq. (39) is dominated by finite $|t|/\hat{s}$, where $\min_{\ell,\hat{s}'} I_t^0$ is at the interception of the $\ell = 2$ and $\ell = 4$ contributions, which can be found by solving a 4th order equation. It leads to

$$\frac{\hat{s}g_{3,1}}{g_{2,0}} \gtrsim -4.9, \quad (40)$$

and it is dominated by the region $t \approx -0.3\hat{s}$, which explains why s-analyticity at large negative $-t \gg m^2$ is necessary. Notice that this is a preliminary result that relies on neglecting higher-order terms. We will come back in the next section to a way (proposed in [45]) to partially circumvent the question of higher-order terms, at least at tree level.
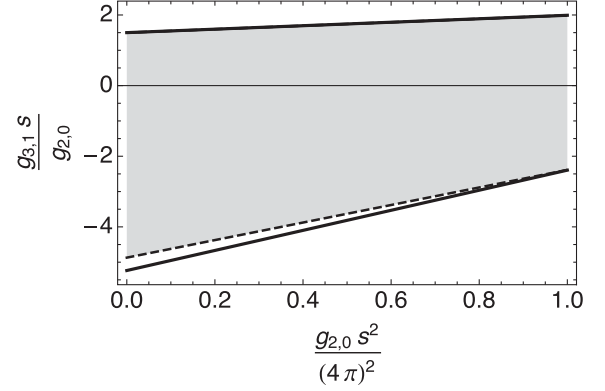
We now turn to loop effects, as captured by Eq. (14). Despite its nonanalyticity, both the amplitude and its first derivative remain finite at all s, t, u within the EFT validity. This is important because the bounds presented in the previous paragraph depend on the first derivative of $a_0(\hat{s}, t)$ at $t = 0$ and on the amplitude at finite $t \approx -0.3\hat{s}$, where loop effects have a finite impact. Ignoring terms at order $(t/\hat{s})^2 \sim (0.3)^2$, loop effects are captured by the substitution,

$$\frac{\hat{s}g_{3,1}}{g_{2,0}} \to \frac{\hat{s}g_{3,1} + \frac{61}{42}\beta_4\hat{s}^2}{g_{2,0} + \frac{\beta_4\hat{s}^2}{2}}, \quad (41)$$

in Eq. (40). We illustrate this in Fig. 3 (the area between the upper solid line and the lower dashed line). Contrary to bounds on moments, here, loop effects have a finite impact on the lower bound, which survives also in the massless limit. In practice, the singularity is regulated, rather than by the mass, by the finite value of t, which happens to determine the lower bound.

A. Resummed higher-order terms

The previous paragraph relies on the approximation that at small $|t| \ll s$, the higher-order terms can be neglected; see Eq. (38). This assumption can be made rigorous using the near forward bounds from [41], which imply that $0 < g_{2n,0}\hat{s}^{2n-2} < g_{2,0}$ and $(2n + 1)g_{2,0}\hat{s}^2/2 > g_{2n+1,1}\hat{s}^{2n+1} > -g_{3,1}\hat{s}$.[7] Alternatively, *at tree level*, higher Wilson coefficients can be eliminated altogether exploiting crossing symmetry, via the "improved" arcs defined in Ref. [45],

---

[7]Notice that, even without crossing symmetry, terms that vanish in the forward amplitude still contribute at loop level to forward arcs and are bounded in absolute value to be smaller than a loop factor times $g_{2,0}$ [8,28].

leading to expressions that are valid for large angle scattering,

$$-t \leq \hat{s} \ll \hat{s}_{\max}, \tag{42}$$

to be contrasted with Eq. (37).

Improved arcs rely on the full $s - t - u$ crossing symmetry of the amplitude to write terms of order $O(t^2)$ or higher as *forward* higher arcs $a_{n \geq 1}(\hat{s}, 0)$ or their first t-derivatives $\partial_t a_{n \geq 1}(\hat{s}, t)|_{t=0}$. These can then be subtracted from both the IR and the UV representation of arcs. The resulting improved arc [45],

$$a_0^{\text{imp}} = a_0(s, t) - \sum_{n \geq 1} (n a_n - \partial_t a_n)|_{t=0}, \tag{43}$$

is defined in the IR and UV by

$$a_0^{\text{imp}}(\hat{s}, t) = g_{2,0} - t g_{3,1} = \frac{2}{\pi} \int_{\hat{s}}^{\infty} \sum_{\ell=0}^{\infty} \frac{d\hat{s}' \text{Im} \hat{f}_\ell(\hat{s}')}{\hat{s}'^3} I_t^{\text{imp}}, \tag{44}$$

with

$$I_t^{\text{imp}} \equiv \frac{(2\hat{s}' + t) P_\ell(\cos\theta)}{2(\hat{s}' + t)^2} - t^2 \left(\frac{3t + 4\hat{s}'}{2(\hat{s}' + t)^2} + \frac{\ell(\ell+1)t}{\hat{s}'^2 - t^2} \right), \tag{45}$$

where $\ell(\ell + 1)$ stems from the derivative of P_ℓ in the forward limit.

We can then proceed as before: For fixed values of $-\hat{s} \leq t \leq 0$, we can find the extrema of I_t^{imp} in $\hat{s}'$ and ℓ. The maximum of I_t^{imp} is discontinuous in t, since for $t < 0$, it is dominated by the (positive) term proportional to $\ell(\ell + 1)$, which diverges as $\ell \to \infty$; at $t = 0$ instead, it is finite and has slope $-3/2$ (saturated by $\ell = 0$ and $\hat{s}' = \hat{s}$). The minimum of I_t^{imp}, similarly to the previous paragraph, is dominated in the interesting region by the interplay of the $\ell = 2$ and $\ell = 4$ polynomials. The result is illustrated in Fig. 4: Improved UV arcs must lie within the allowed (nongray) region for all values of t.

At tree level, a comparison with the (now) exact IR arc Eq. (44) leads to

$$\frac{3}{2} > \hat{s} \frac{g_{3,1}}{g_{2,0}} \gtrsim -5.18, \tag{46}$$

compatibly with [42,43,45,46].[8] Notice that this bound appears weaker than the nonimproved one Eq. (40), which ignored $O(t^2)$ terms.

---

[8]In this approach, we have not included higher null constraints.

The tree-level improved bound appears to be somewhat sharper, since higher-order tree-level Wilson coefficients have been eliminated exactly from both IR and UV parts of the dispersion relation. Once IR effects are taken into account, however, these higher-order Wilson coefficients reappear into arcs. For instance, while the term $\propto g_{4,0}$ is canceled from $a_0(\hat{s}, t) - 2t^2 a_1(\hat{s}, 0) - 3t^4 a_2(\hat{s}, 0) - \cdots$, there is a loop effect $\propto g_{2,0} g_{4,0}/16\pi^2$ that does not cancel. It is not possible to eliminate $g_{4,0}$ altogether from $a_0(\hat{s}, t)$.

So, contrary to tree-level arcs that could be improved into compact expressions involving a finite number of Wilson coefficients, loop level effects propagate all order coefficients into arcs. We will have to assume that these terms are small for all values of s at which we evaluate bounds. We express this assumption as $\hat{s} \ll \hat{s}_{\max}$ in Eq. (42).

Under this assumption, we can focus on the most relevant term, discussed already in Eq. (12), and compute the improved arc using the algorithm Eq. (43). In addition to the first expression in Eq. (44), we find

$$\delta a_0^{\text{imp}} = \frac{g_{2,0}^2}{16\pi^2} \left(\frac{-21s^2 + 61ts + t^2 \log\left(1 - \frac{s}{t}\right)}{60} - \frac{2t^3}{3s} \right), \tag{47}$$

instead of the nonimproved version Eq. (14). Including this term in the EFT, we can rederive the bound Eq. (46), which we show as the solid line in Fig. 4. The improved result is very similar to the approximated one.

Importantly, the improvement algorithm Eq. (43) involves higher arcs and their first derivatives at $t \to 0$. As argued in Eq. (14), these are finite, despite being evaluated in the forward kinematics. This result is not a priori obvious. Moreover, thank to Eq. (16), it extends also to improvements of higher arcs. Indeed, consider for example $g_{6,2}$. The necessary improvement [the analog of Eq. (44)] to eliminate all terms $g_{n,2}$, $n > 6$ from $a_1(\hat{s}, t)$ involves now second derivatives of higher arcs at $t = 0$, $\partial_t^2 a_n(\hat{s}, t)|_{t=0, n \geq 2}$. Equation (16) implies that these are all regular. More generally, terms $\propto (stu)^q$ in Eq. (8), appear
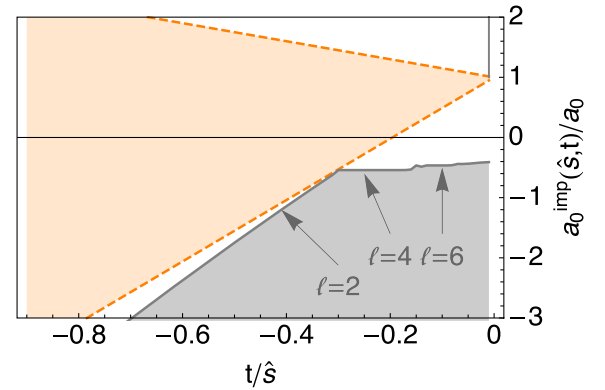

FIG. 4. As in Fig. 2, but using improved arcs $a_0^{\text{imp}}(\hat{s}, t)$, and comparison with the now exact expression Eq. (44) (orange) with extremal values given in Eqs. (46).

first in arc $a_{q-1}(\hat{s}, t)$ (see footnote 1). Its improved version requires $\partial^q|_{t=0} a_n(\hat{s}, t), n \geq q$, which is regular according to Eq. (16).

These results give strength to the methods pioneered in [45]: Although designed for tree-level amplitudes, they hold also at loop level for the simple scalar theory with no gravity that we have considered in this work.

V. CONCLUSIONS AND OUTLOOK

We have studied the impact of calculable IR loop effects on EFT positivity bounds, focusing on the effect of IR singularities in the massless limit. This largely extends the initial investigations in [40,41], which focused on IR-finite contributions as running effects. The role of IR-sensitive loop correction studied in the present work is actually more relevant for bounds relying on full crossing symmetry of the amplitude [42,43], such as the lower bound on the coefficient ratio $g_{3,1}\hat{s}/g_{2,0}$. The singular behavior stems from a tension between the need of probing the EFT at large enough energies $\hat{s}$, where bounds on Wilson coefficients are stronger and small enough t where the amplitude is analytic.

If s-analyticity of the amplitude is granted only for a limited range of values taken by t, $|t| \lesssim m^2$, we have shown how to extract the bounds, extending the approach of [41] to the 2D moment problem, as in [46]. One-loop effects involving marginal couplings $\lambda\phi^4$ have no qualitative impact on the bounds. On the other hand, loops involving the coupling $g_{2,0}$ induce a $\log m^2/\hat{s}$ divergence in the derivative of the arcs, which invalidates the bound for $m \to 0$. Since $g_{2,0}$ and $g_{3,1}$ do not run, the divergence is physical.

If instead the amplitude is analytic also for large negative t, then all the bounds are robust. We have shown this by introducing a novel and simple analytic understanding of dispersion relations at finite t (which complement the numerical approach of [45]), represented by the *trumpet* in Fig. 2, which can be applied to any amplitude regular in the forward limit. In this approach, the upper bound on $g_{3,1}$ is shown to be dominated by the dispersion relation at $t/\hat{s} \approx -0.3$, where the above singularities are absent. Moreover, this approach makes little use of crossing symmetry, whose practical purpose is to guarantee that the higher-order coefficients $g_{n,1}(n > 4)$ are bounded by the lower coefficients. It would be interesting to bring this analytic approach into a more systematic tool to approach all bounds.

Moreover, the improvement procedure that removes higher-order terms still relies on evaluating infinitely many dispersion relations in the forward limit. We have studied the structure of all one-loop effects in the scalar theory and found that, interestingly, all the necessary forward limits are regular. It would be interesting to repeat this analysis in more complex theories, including ϕ^3, flavor, or gravity, to establish the robustness of this mixed forward and non-forward procedure. Moreover, the study of higher loops of more relevant couplings as well theories with exactly massless particles, such as Yang-Mills theory, might reveal more singular behaviors. Overall, it would be useful to develop an improvement procedure without the forward limit.

APPENDIX: DISCRETE MOMENTS

Treating the distribution in J^2 as continuous gives a convenient and manageable way to setting conservative constraints on the arcs without having to truncate the expansion in Legendre polynomials P_ℓ up to some $\ell_{\max}$. However, we remark that it excludes polynomials that might be negative between integer values of ℓ, so the bounds are not optimal. In [46], the condition is imposed via a set of positive determinants. In this appendix, we propose a simple way to systematically improve the bounds.

The two-dimensional moments,

$$\mu_n^j = \frac{2}{\pi} \int_s^\infty \frac{ds}{s} \mathrm{Im} f_\ell(s) \sum_\ell \frac{(\ell(\ell+1))^j}{s^{n+2}}, \quad \text{(A1)}$$

can be split as a sum of two terms,

$$\mu_n^j = \sum_\ell^{L-1} (\ell(\ell+1))^j \frac{2}{\pi} \int_s^\infty \frac{ds}{s} \mathrm{Im} f_\ell(s) \frac{1}{s^{n+2}} \quad \text{(A2)}$$

$$+ \frac{2}{\pi} \int_s^\infty \frac{ds}{s} \int_{L(L+1)}^\infty f(J^2, s) \frac{(\ell(\ell+1))^j}{s^{n+2}}. \quad \text{(A3)}$$

In the first term, we are considering the two-dimensional moment problem in a grid of L sites, each site being a one-dimensional moment problem with a different measure $\mathrm{Im} f_\ell(s)$. This automatically imposes the constraints for all moments above $j > L$.

The grid in J^2 is specified by the zeroes of

$$g(J^2) = \prod_{i=0}^{L-1} (J^2 - i(i+1)), \quad \text{(A4)}$$

and gives a relation between L different moments. Explicitly, for $L = 2$, $g(J^2) = J^2(J^2 - 2)$ and $\mu_n^{j+2} - 2\mu_n^{j+1} = 0$, so there are only two (L, in general) independent moments in j, μ_n^0 and μ_n^1. Writing the two-dimensional problem as continuous and then imposing the grid constraints in Eq. (A4) is equivalent of considering L different one-dimensional problems. We find more convenient using the latter since, besides being more physical, one can impose the upper bound on the partial waves $\mathrm{Im}f_\ell \leq 16\pi(2\ell + 1)$,

$$\frac{2}{\pi} \int_s^\infty \frac{ds}{s} \frac{\mathrm{Im}f_\ell(s)}{s^{n+2}} < \frac{1}{s^{n+2}} \frac{32(2\ell + 1)}{n + 2}. \quad \text{(A5)}$$

The second term in Eq. (A2) is the two-dimensional moment problem already described in the main text. Notice that now the domain is given by

$$x \geq 0, \qquad 1 - x \geq 0, \qquad J^2 - L(L + 1) \geq 0, \quad \text{(A6)}$$

instead of Eq. (24). This maintains information for asymptotic partial waves, and the approximation of not considering negative polynomials between ℓ above L is extremely good already for relatively low $L \sim 4$ in the examples considered if numerical precision is desired, but setting $L = 0$ as done in the main text allows for a simple and accurate analytical understanding.

[1] T. N. Pham and T. N. Truong, Phys. Rev. D **31**, 3027 (1985).

[2] B. Ananthanarayan, D. Toublan, and G. Wanders, Phys. Rev. D **51**, 1093 (1995).

[3] M. R. Pennington and J. Portoles, Phys. Lett. B **344**, 399 (1995).

[4] A. Adams, N. Arkani-Hamed, S. Dubovsky, A. Nicolis, and R. Rattazzi, J. High Energy Phys. 10 (2006) 014.

[5] B. Bellazzini, J. High Energy Phys. 02 (2017) 034.

[6] C. de Rham, S. Melville, A. J. Tolley, and S.-Y. Zhou, J. High Energy Phys. 03 (2018) 011.

[7] L. Vecchi, J. High Energy Phys. 11 (2007) 054.

[8] A. Nicolis, R. Rattazzi, and E. Trincherini, J. High Energy Phys. 05 (2010) 095; 11 (2011) 128(E).

[9] B. Bellazzini, L. Martucci, and R. Torre, J. High Energy Phys. 09 (2014) 100.

[10] C. de Rham, S. Melville, A. J. Tolley, and S.-Y. Zhou, Phys. Rev. D **96**, 081702 (2017).

[11] J. Distler, B. Grinstein, R. A. Porto, and I. Z. Rothstein, Phys. Rev. Lett. **98**, 041601 (2007).

[12] A. V. Manohar and V. Mateu, Phys. Rev. D **77**, 094019 (2008).

[13] I. Low, R. Rattazzi, and A. Vichi, J. High Energy Phys. 04 (2010) 126.

[14] A. Falkowski, S. Rychkov, and A. Urbano, J. High Energy Phys. 04 (2012) 073.

[15] B. Bellazzini, F. Riva, J. Serra, and F. Sgarlata, J. High Energy Phys. 11 (2017) 020.

[16] B. Bellazzini and F. Riva, Phys. Rev. D **98**, 095021 (2018).

[17] C. Zhang and S.-Y. Zhou, Phys. Rev. D **100**, 095003 (2019).

[18] G. N. Remmen and N. L. Rodd, J. High Energy Phys. 12 (2019) 032.

[19] B. Bellazzini, F. Riva, J. Serra, and F. Sgarlata, J. High Energy Phys. 10 (2019) 189.

[20] C. Englert, G. F. Giudice, A. Greljo, and M. Mccullough, J. High Energy Phys. 09 (2019) 041.

[21] T. Trott, J. High Energy Phys. 07 (2021) 143.

[22] Q. Bonnefoy, E. Gendy, and C. Grojean, J. High Energy Phys. 04 (2021) 115.

[23] J. Davighi, S. Melville, and T. You, J. High Energy Phys. 02 (2022) 167.

[24] M. Chala and J. Santiago, Phys. Rev. D **105**, L111901 (2022).

[25] A. Azatov, D. Ghosh, and A. H. Singh, Phys. Rev. D **105**, 115019 (2022).

[26] A. Gruzinov and M. Kleban, Classical Quantum Gravity **24**, 3521 (2007).

[27] B. Bellazzini, C. Cheung, and G. N. Remmen, Phys. Rev. D **93**, 064076 (2016).

[28] B. Bellazzini, F. Riva, J. Serra, and F. Sgarlata, Phys. Rev. Lett. **120**, 161101 (2018).

[29] Y. Hamada, T. Noumi, and G. Shiu, Phys. Rev. Lett. **123**, 051601 (2019).

[30] C. de Rham, S. Melville, A. J. Tolley, and S.-Y. Zhou, J. High Energy Phys. 03 (2019) 182.

[31] L. Alberte, C. de Rham, A. Momeni, J. Rumbutis, and A. J. Tolley, J. High Energy Phys. 03 (2020) 097.

[32] B. Bellazzini, M. Lewandowski, and J. Serra, Phys. Rev. Lett. **123**, 251103 (2019).

[33] S. Kim, T. Noumi, K. Takeuchi, and S. Zhou, J. High Energy Phys. 12 (2019) 107.

[34] J. Tokuda, K. Aoki, and S. Hirano, J. High Energy Phys. 11 (2020) 054.

[35] M. Herrero-Valea, R. Santos-Garcia, and A. Tokareva, Phys. Rev. D **104**, 085022 (2021).

[36] Z. Bern, D. Kosmopoulos, and A. Zhiboedov, J. Phys. A **54**, 344002 (2021).

[37] X. O. Camanho, J. D. Edelstein, J. Maldacena, and A. Zhiboedov, J. High Energy Phys. 02 (2016) 020.

[38] N. Afkhami-Jeddi, S. Kundu, and A. Tajdini, J. High Energy Phys. 04 (2019) 056.

[39] B. Bellazzini, G. Isabella, M. Lewandowski, and F. Sgarlata, J. High Energy Phys. 05 (2022) 154.

[40] N. Arkani-Hamed, T.-C. Huang, and Y.-T. Huang, J. High Energy Phys. 05 (2021) 259.

[41] B. Bellazzini, J. Elias Miró, R. Rattazzi, M. Riembau, and F. Riva, Phys. Rev. D **104**, 036006 (2021).

[42] A. J. Tolley, Z.-Y. Wang, and S.-Y. Zhou, J. High Energy Phys. 05 (2021) 255.

[43] S. Caron-Huot and V. Van Duong, J. High Energy Phys. 05 (2021) 280.

[44] A. Sinha and A. Zahed, Phys. Rev. Lett. **126**, 181601 (2021).

[45] S. Caron-Huot, D. Mazac, L. Rastelli, and D. Simmons-Duffin, J. High Energy Phys. 07 (2021) 110.

[46] L.-Y. Chiang, Y.-t. Huang, W. Li, L. Rodina, and H.-C. Weng, J. High Energy Phys. 03 (2022) 063.

[47] J. Henriksson, B. McPeak, F. Russo, and A. Vichi, J. High Energy Phys. 06 (2022) 158.

[48] A. Nicolis, R. Rattazzi, and E. Trincherini, Phys. Rev. D **79**, 064036 (2009).

[49] M. Froissart, Phys. Rev. **123**, 1053 (1961).

[50] A. Martin, Phys. Rev. **129**, 1432 (1963).

[51] Y. S. Jin and A. Martin, Phys. Rev. **135**, B1375 (1964).

[52] A. Martin, Nuovo Cimento A **42**, 930 (1965).

[53] A. Martin, *Scattering Theory: Unitarity, Analyticity and Crossing* (Springer Berlin, Heidelberg, 1969), Vol. 3.

[54] G. Sommer, Fortschr. Phys. **18**, 577 (1970).

[55] J. Lasserre, *Moments, Positive Polynomials and Their Applications*, Series on Optimization and its Applications: Volume 1 (Imperial College Press, 2009), 10.1142/p665.

[56] K. Schmüdgen, Math. Ann. **289**, 203 (1991).

[57] A. Guerrieri and A. Sever, Phys. Rev. Lett. **127**, 251601 (2021).

[58] M. F. Paulos, J. Penedones, J. Toledo, B. C. van Rees, and P. Vieira, J. High Energy Phys. 11 (2017) 133.

[59] M. F. Paulos, J. Penedones, J. Toledo, B. C. van Rees, and P. Vieira, J. High Energy Phys. 11 (2017) 143.

[60] M. F. Paulos, J. Penedones, J. Toledo, B. C. van Rees, and P. Vieira, J. High Energy Phys. 12 (2019) 040.

[61] J. Bros, H. Epstein, and V. Glaser, Commun. Math. Phys. **1**, 240 (1965).